Analytica Chimica Acta 1107 (2020) 135–144

Contents lists available at ScienceDirect

Analytica Chimica Acta

journal homepage: www.elsevier.com/locate/aca

DNA aptamer-based non-faradaic impedance biosensor for detecting *E. coli*

Gaser N. Abdelrasoul [a], Afreen Anwar [a, b], Scott MacKay [a], Marcus Tamura [a], Manzoor A. Shah [b], Damase P. Khasa [c], Ruth R. Montgomery [d], Albert I. Ko [e], Jie Chen [a, *]

[a] Electrical, and Computer Engineering Department, University of Alberta, Edmonton, AB, Canada
[b] Department of Botany, University of Kashmir, Srinagar, 190006, J&K, India
[c] Centre for Forest Research (CEF), Institute for Integrative and Systems Biology (IBIS), and Canada Research Chair in Forest and Environmental Genomics, Université Laval, Québec, QC, G1V0A6, Canada
[d] Internal Medicine, Yale School of Medicine, New Haven, CT, 06520, USA
[e] Department of Epidemiology of Microbial Diseases, School of Public Health, Yale University, New Haven, CT, 06510, USA

HIGHLIGHTS

- A real-time lab-on-chip design to detect *E. coli* with the detection limit of 9 cfu mL^{-1}.

ARTICLE INFO

Article history:
Received 23 September 2019
Received in revised form
31 January 2020
Accepted 2 February 2020
Available online 7 February 2020

Keywords:
E. coli
Electrochemical biosensor
Aptamer-based sensor
Water quality monitoring and environmental sensor

ABSTRACT

Developing a real-time, portable, and inexpensive sensor for pathogenic bacteria is crucial since the conventional detection approaches such as enzyme-linked immunosorbent assay (ELISA) and polymerase chain reaction (PCR) assays are high cost, time-consuming, and require an expert operator. Here we present a portable, inexpensive, and convenient impedance-based biosensor using Interdigitated Electrode (IDE) arrays to detect *Escherichia coli* (*E. coli*) as a model to demonstrate the feasibility of an impedance-based biosensor. We manipulated the affinity of the IDE array towards *E. coli* (*E. coli* BL21 series) by functionalizing the IDEs' surface with an *E. coli* outer membrane protein (OMP) Ag1 Aptamer. To determine the dominant factors affecting the sensitivity and the performance of the biosensor in detecting *E. coli*, we investigated the roles of the substrate material used in the fabrication of the IDE, the concentration of the aptamer, and the composition of the carboxy aliphatic thiol mixture used in the pretreatment of the IDE surface. In the sensing experiments we used an *E. coli* concentration range of 25 −1000 cfu mL^{-1} and confirmed the binding of the OMP Ag1 Aptamer to the outer membrane protein of the *E. coli* by Field Emission Scanning Electron Microscopy (FESEM), Optical Microscopy, and Atomic Force Microscopy (AFM). By tuning the surface chemistry, the IDEs' substrate material, and the concentration of the OMP Ag1 Aptamer, our sensor could detect *E. coli* with the analytical sensitivity of approximately 1.8 Ohm/*cfu* and limit of detection of 9 cfu mL^{-1}. We found that the molecular composition of the self-assembled monolayer (SAM) formed on the top of the IDEs before the attachment of the OMP Ag1 Aptamer significantly impacted the sensitivity of the sensor. Notably, with straightforward changes to the molecular recognition elements, this platform device can be used to detect a wide range of other microorganisms and chemicals relevant for environmental monitoring and public health.

1. Introduction

Sensing of microorganisms by probing the impedance variation of their interaction with surface functionalized interdigitated electrode arrays (IDEs) is emerging as a fast, inexpensive, and highly accurate technique. IDEs are particularly favored for this purpose due to their tractability in surface chemistry engineering, the versatility of materials used in fabrication, electrode design, and capability for hand-held sensing applications. IDE based sensors

* Corresponding author.
E-mail address: jc65@ualberta.ca (J. Chen).

https://doi.org/10.1016/j.aca.2020.02.004
0003-2670/

have been widely used in several fields such as biomedical sensing [1,2], environmental sensing [3,4], and optoelectronics [5]. Several trials have been conducted to utilize IDEs in building sensors to detect microorganisms [6–10], but most are not practical due to the use of highly sensitive biomolecules, which is difficult to handle onsite or the complexity of detection mechanisms. Due to the risks that microorganisms, and due to their waterborne and foodborne nature, it is crucial that an effective detection system be available. *Escherichia coli* (*E. coli*) present pervasively in the abdominal of animals, but disease manifestations caused by infection of *E. coli* pathogenic variants can range from mild fevers and diarrhea to severe dehydration and death. Conventional detection approaches such as enzyme-linked immunosorbent assay (ELISA) and polymerase chain reaction (PCR) assays can be expensive, time-consuming, and required a well-trained operator. Such a portable detection system for *E. coli* would be beneficial for a variety of fields, including clinical, public health, industrial (food, beverage, and catering), municipal water monitoring, and environmental monitoring.

The ubiquitous spread of *E. coli* has attracted research into detection systems, and several detection techniques that aim to improve the sensitivity and lower the analysis cost have been proposed [11–13]. Electrochemical biosensors [14–16], optical [17–21], and bioanalytical immunoassay [22,23] approaches were applied to detect *E. coli* in different media, including municipal water, food products, and agricultural products. Generally, the biosensor procedures are precise, time-effective, and vital in the prevention and diagnosis of bacterial diseases. Biosensors represent the combination of a range of versatile technologies and eliminate the shortcoming linked with PCR techniques. In the electrochemical biosensors, the identification of the *E. coli* performed either through an electrochemical cell consisting of three electrodes that are immersed in an electrolyte solution [24–27], or IDEs with a minimum amount of measuring solution, easy handling, and capabilities for incorporating into portable devices [28–30]. The sensing of the *E. coli* using electrochemical cell biosensors based on either amperometric or an impedance mechanism to follow the change in the bacterial concentration, where the methodology of the sensing mainly depends on the probe and the material of the electrode. The potentiostat electrochemical cell used in biosensing of *E. coli* consists of building three electrodes: a working electrode, a counter electrode, and a reference electrode. The fabrication process of the working electrode introduces complexity, especially when nanomaterials are used to increase the electrodes' surface area and chemical activity. For instance, an electrochemical biosensor to detect *E. coli* O157:H7 was developed by using biofunctionalized polymeric nanocomposite beads to separate and probe the bacteria in food samples [31]. By following the cyclic voltammetric diagram, *E. coli* could be detected down to a concentration of 10^2 *cfu* mL^{-1}. The sensing mechanism, however, is complicated as the preparation of the probe and the transducer consists of several steps. To improve the sensitivity of electrochemical cell-based biosensors, multiple signal amplification steps are necessary, where enzymatic amplification with redox cycling accompanied with charge transfer process was employed using Hydroquinone Diphosphate as an active substrate obtaining a sensitivity range of 10^3 to 10^8 *cfu* mL^{-1} [32]. However, sensing of *E. coli* based on an electrochemical cell with acceptable sensitivity and detection limits requires multiple steps of electrode surface modification, complex instrumentation setup, and several signal amplification steps.

Aptamers are short, single-stranded DNA, RNA, or synthetic XNA molecules that can specifically bind to any desired targets with high affinity [33]. Recently, different aptamers have been successfully isolated and employed to detect different strains of *E. coli* using several techniques such as optical, fluorescent-tag, and electrochemical [34,35]. The main benefit of using aptamer to target *E. coli* in addition to the high selectivity is that the aptamer is more environmentally stable and can be stored and handled without strict precautions as in the case of other biomarkers.

Over the past years, we have developed a portable impedance-based biosensing system, which consists of interdigitated electrodes (IDEs) with surface functionalized biorecognition elements, the impedance measurement portable board, and developed reading and analyzing software. We studied the theoretical and the practical prospects of the non-faradaic impedance sensing, the pivotal factors that impact on the electrical field between the electrode and therefore, the sensitivity of the sensor, and published our findings elsewhere. Here, we develop a portable non-faradaic impedance-based biosensor for detecting *E. coli* employing a label-free DNA aptamer as a probe and an IDE chip as a transducer. We utilize *E. coli* OMP Ag1 oligonucleotide Aptamer targeting the outer membrane protein of the *E. coli* as a biorecognition probe, and carboxy aliphatic thiol compounds as an activated linker to bind the probe to IDE surfaces. *E. coli* BL21 and *Shigella flexneri* were selected to be the analyte and the negative control bacteria, respectively, across the study. We evaluated the impact of the IDEs' substrate material on the sensitivity of the biosensor by testing silicon dioxide coated silicon wafers and borofloat glass wafers as substrates for the IDE across a range of *E. coli* concentrations and measuring the response. We also assessed different combinations of carboxy aliphatic thiol compounds with different aliphatic chain lengths to activate the gold surface of the IDE to capture the *E. coli* OMP Ag1 aptamer and investigated the effect of their monolayer molecular surface assembly behavior on the sensitivity of the biosensors. To achieve that mercaptoundecanoic acid (11-MUA), mercaptohexadecanoic acid (16-MDA), and mixtures of different ratios of both were used to functionalize the gold surface of the IDE before the anchoring of the aptamer, while the final molar concentration of the thiol compound or mixture was kept at 10 mM. The formed self-assembled monolayer (SAM) of the carboxy aliphatic thiol compound renders the gold surface of the IDEs coated with the carboxylic groups facilitating the attachment of the aptamer through EDC/NHS chemistry. We aim to create an inexpensive, sensitive, reagent-free, and easy-to-use biosensor for detecting *E. coli* in water bodies, potable water, and food samples, which provides a portable biomonitoring system serving different fields such as environmental monitoring, pharmaceutical, and food safety. The advantages of our method over the traditional PCR, or ELISA are low-cost, portable, and easy-to-use. Before measuring the impedance to detect the *E. coli*, we pre-functionalized the IDE chip with the recognition element, and thus no need for other steps of treatment or amplification. On the other hand, in the case of the ELISA method, the detection of the target *E. coli* consists of multi-steps procedure including the adding of the detection recognition element, the substrate, and the stop solution, where each step could take more than an hour to accomplish. The costs of PCR or ELISA reagents and the instrumentation are higher than our device (about $1 per test). Figure 1 presented our point-of-care biosensor, which consists of electronic reader board in housing unit, disposable IDE chip with connector, and analyzing application software on smartphone or tablet.

2. Results and discussion

2.1. Surface functionalization of IDE

The fabricated IDE chip consists of eight electrodes, as shown in Fig. 1, and we covered with PDMS cover that has eight wells one for each electrode to separate the liquid in contact with the electrode,

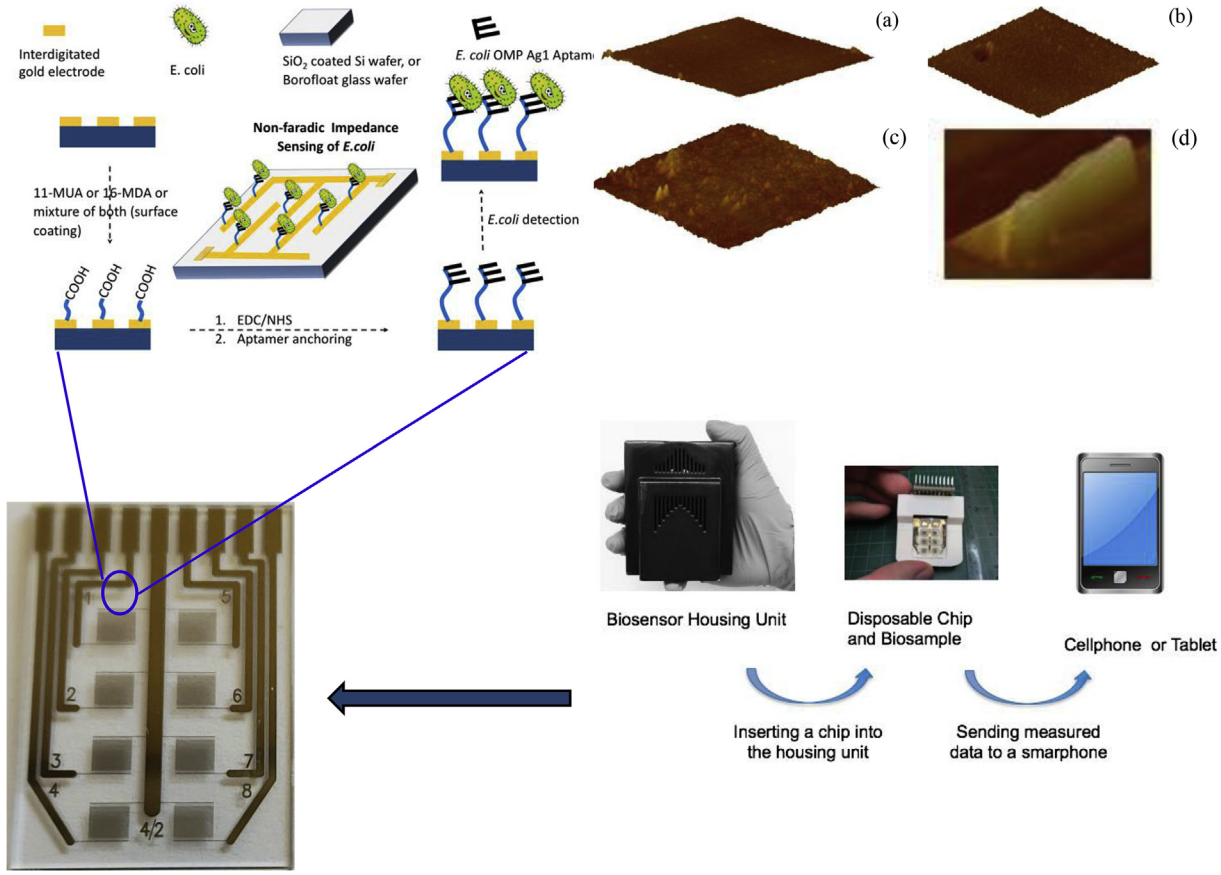

Fig. 1. (Bottom Right) represented the components of our portable point-of-care biosensor, which consists of biosensor housing unit contained the electronic circuit reader, disposable chip and biosampler, and cellphone or tablet to run the analytical software. (**Bottom Left**) showed the digital image of the IDE chip made using a glass substrate. We fabricated the IDE chip with the same design using SiO_2 coated silicon substrate. The IDE chip has eight microelectrode arrays each is of 3 mm^2 dimensions and contains 168 digit pairs with 4 μm and 2 μm, finger width, and separation gap, respectively. **(Top Left)** Representation of the steps involved in the surface modification of the IDEs with *E. coli* OMP Ag1 Aptamer to detect *E. coli*. The functionalization occurred at the surface of the gold electrode digits by forming a SAM of Carboxy aliphatic thiol molecules to facilitate the attachment of the *E. coli* OMP Ag1 probe. The anchored probe is capable of capturing the *E. coli* through the attachment to their outer protein membrane. (**Top Right**) AFM micrographs of an IDE array at different surface modification stages were taken at 3 μm [2] surface plot on a gold digit, (a) bare gold electrode, (b) MUA surface coated electrode, (c) *E. coli* OMP Ag1 aptamer coated MUA functionalized electrode, and (d) *E. coli* BL21 spotted on the top of the functionalized electrode.

which allows running eight experiments at the same time. Each electrode is 3 mm^2 dimensions and contains 168 digit pairs of 4 μm width and 2 μm separation gap between fingers. After cleaning the IDE and before outfitting the IDE for *E. coli* sensing, we measured the impedance magnitude of each electrode by placing the measuring buffer in PDMS well on the top of the electrode and called it the baseline. Building IDE sensitive to *E. coli* consists of two steps: formation of a self-assembled monolayer (SAM) of carboxy aliphatic thiol compounds, and anchoring of the bio-probe (*E. coli* OMP Ag1) as represented in the schematic diagram in Fig. 1 (Left). First, we form a SAM on the gold electrode digits using 11-MUA, or 16-MDA, or different combinations of both of them. The formation of the SAM occurred based on the affinity of the thiol groups to the gold surfaces leaving the carboxylic group facing the solution for the next step. Second, we activate the carboxylic groups of the carboxy aliphatic thiol compounds with EDC and NHS reagents to enable the coupling with the amine groups terminating the *E. coli* OMP Ag1 Aptamer molecules in aqueous solution. Then we add the *E. coli* OMP Ag1 Aptamers to the activated IDEs, which are anchored by an amide linkage to the surface of the gold electrode digits. We employed AFM to follow the surface functionalization of the IDEs at each step, where we imaged the surface of the gold electrode digits in a 3 μm^2 area and evaluated the change in the topographic roughness. The sputtering technique used in the microfabrication of the IDEs chip produced smooth gold electrode digits with roughness around 3 nm, as depicted in Fig. 1(a). The formation of the SAM on the gold digits raised the roughness to 5 nm when 11-MUA of 10 mM was used as a carboxy aliphatic thiol reagent Fig. 1(b). We found the topography of the formed SAM significantly changed with the composition of the carboxy aliphatic thiol mixture as discussed later on. By functionalizing the gold electrode digits with the *E. coli* OMP Ag1 aptamer molecules the roughness jumped up to 9 nm, while the attachment of the *E. coli* extremely boosted the roughness to around 500 nm and sometimes exceeded the threshold of the AFM tip as seen in Fig. 1(d). The increment in the roughness, along with the progress in the functionalization of the gold electrode digits gives a clue on the effectiveness of the surface modification steps.

The attachment of the *E. coli* to the gold electrode digits via the *E. coli* OMP Ag1 aptamer probe was further confirmed by FESEM, as shown in Fig. 2(a). The selective functionalization of the gold electrode digits led all of the *E. coli* cells to be attached to the surface of the electrode digits. We did not observe any *E. coli* adherence to the silicon dioxide surface between the digits. Some of the *E. coli* cells were found trapped in between the electrode digits, but by going to high magnification, the *E. coli* cells were observed to have

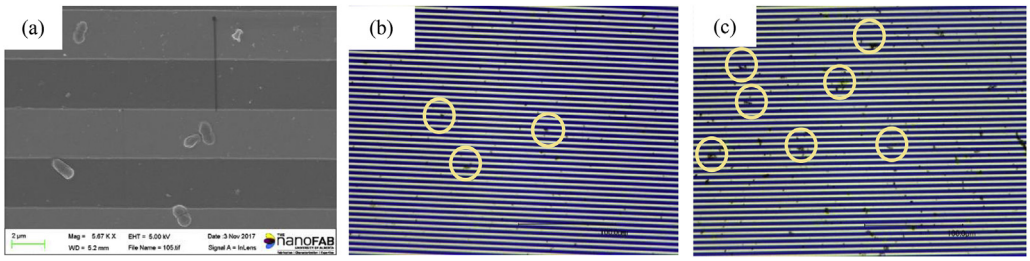

Fig. 2. (a) FESEM images of fully functionalized IDEs after spotting with *E. coli* of 250 cfu mL^{-1} concentration, (b) and (c) are optical microscope images of the E-coli OMP Ag1 aptamer surface coated IDEs substrates that were spotted with 50 and 500 cfu mL^{-1} E. *coli*, respectively, the scale bar in both optical microscopy images is 100 μm. Yellow circles assign the *E. coli* bacteria. (For interpretation of the references to colour in this figure legend, the reader is referred to the Web version of this article).

adhered through their outer protein membrane to the edge of the electrode digits and settled on the silicon dioxide base substrate, as further depicted in Figs. S1 and S2 in the supporting information. We also employed an optical microscope to scrutinize the distribution of the *E. coli* on the electrode digits precoated with *E. coli* OMP Ag1 aptamer. Fig. 2(b) and 2(c) show optical microscope images of the IDEs with two different concentrations of *E. coli* cells, 50 and 500 cfu mL^{-1}, respectively. *E. coli* cells were homogeneously distributed covering the IDEs without any observed aggregation at a lower concentration, while some aggregates with sizes of 10–15 μm were observed at a higher concentration. The change in the impedance magnitude (Z) with the surface functionalization of the IDE provides a tool to verify the attachment of the functional group, whereby comparing with the baseline impedance magnitude, we noticed a change in the Z profile with each step of functionalization as well as after the addition of the bacteria (*E. coli or Shigella flexneri*). Fig. 3(a) and 3(b) showed the Z profiles for IDEs made with SiO_2 coated and glass substrates, respectively, at various stages of surface functionalization and after the addition of the *E. coli* (500 cfu mL^{-1}), where Fig. 3(c) presented the Z profiles in the case of the *Shigella flexneri* (the negative control). By comparing with the Z profile of the baseline, the Z constantly increased with the attachment of MUA and the aptamer before decreased with the attachment of the *E. coli* or *Shigella flexneri* bacteria. We found that the degree of the reduction in the Z associated with the attachment of the bacteria is proportional to the concentration of the bacteria in the tested solution in the case of *E. coli*, but was neglected in the case of *Shigella flexneri* bacteria regardless the concentration of the bacteria, which demonstrated the specificity of the aptamer-probe. Electrically, *E. coli* cells act as capacitors. *E. coli* consists of a conductive cytoplasm with other conductive periplasm separating two insulating cell membranes giving dielectric properties to the *E. coli* cell, which explained the decrease in the Z with the attachment of the *E. coli* and was intensively studied [28,36]. The impact in the non-faradaic impedance spectra by the attachment of *E. coli* cells to the IDEs surface can be utilized to detect the presence of the bacteria in the solution as well as the bacteria concentration. We calculated the difference in the Z (ΔZ) of each consecutive stage of surface functionalization at 10 kHz in Fig. 3(a), 3(b), and 3(c) and presented in Fig. 3(d). In the case of IDE made from SiO_2 coated substrate, the ΔZ caused by the alteration in the surface functionality of the IDEs is about 200 Ohm, while it is about 1200 Ohm caused by the attachment of the *E. coli* (500 cfu mL^{-1} bacteria concentration), and that indicates the attachment of the *E. coli* dominates the change in the non-faradaic impedance of the IDE. By moving to IDE made using the glass substrate, the ΔZ caused by the attachment of the *E. coli* using the same concentration of the bacteria solution (500 cfu mL^{-1}) was around 500 Ohm, which reveals that the IDE's substrate material has a significant impact on determining the sensitivity of the sensor. When we used the *Shigella flexneri* solution with 500 cfu mL^{-1} concentration, the ΔZ resulted from the attachment of the bacteria was 89 Ohm, which is less than that caused by the surface functionalization of the IDE (161 and 128 Ohm). These ΔZ values and by comparing them with that obtained with *E. coli* bacteria show that the attachment of the *Shigella flexneri* bacteria to the IDE functionalized with the *E. coli* OMP Ag1 aptamer was insignificant, which indicates the high specificity of the fabricated sensor. To evaluate the latency of the binding of *E. coli* BL21 with the *E. coli* OMP Ag1 aptamer, we ran a simple reaction (bio-recognition) time experiment, where we measured the variation in the ΔZ faradaic at different incubation times over the precoated IDEs. After the addition of the *E. coli*, we measured the impedance magnitude every 30 min in the frequency range from 1 kHz to 1 MHz. The ΔZ was calculated by comparing the measurements with the measurements taken before adding the *E. coli* at 10 kHz. Fig. 3(e) represents the variation in the ΔZ with time, where it becomes notable after 60 min of *E. coli* incubation. The increment in the ΔZ continues in a step manner until 180 min of incubation, where after that it slightly increases, which might indicate the reaching of the bio-recognition equilibrium. We continued measuring the change in the impedance up to 240 min. However, we did not observe any noticeable change after 180 min.

2.2. The effect of the E. coli OMP Ag1 aptamer concentration

A wide range of aptamer concentrations from 2×10^{-3} to 0.2 μM has been used in the electrochemical-based methods for the detection of *E. coli* using OMP aptamers as a probe [37,38]. To optimize the concentration of the *E. coli* OMP Ag1 aptamer for the IDEs coating, we selected three concentrations (2.5, 5, and 10 μM) of the aptamer for use during the surface functionalization of the IDEs resulting in three IDEs coated with three different aptamer concentrations. By following the feedback of each IDE toward a series of *E. coli* cell concentrations (from 25 to 1000 cfu mL^{-1}) and comparing the difference of the impedance magnitudes before and after the *E. coli* cells addition (ΔZ), we estimated the sensitivity of the IDE biosensor. The sensitivity of the IDE sensor toward the *E. coli* can be estimated from the slope of the ΔZ with the change in the *E. coli* cells concentration. At lower *E. coli* cell concentrations (below 200 cfu mL^{-1}), the IDEs coated with 2.5 μM aptamer shows an enormous increase in the ΔZ with increasing *E. coli* concentration as indicated by the dashed circle in Fig. 4 ((a), the black square). However, the situation is reversed at higher concentrations of *E. coli* cells, where the value of ΔZ decreases with increasing *E. coli* concentration giving the slope of 0.13 Ohm/(*cfu*.mL^{-1}), which represents the sensitivity of the IDE toward the *E. coli*. The decrease in the ΔZ could be due to saturation of the aptamer-probe at higher *E. coli* cells concentrations which prevent the IDEs from capturing more cells and consequently prevents the detection of changes in the concentration of the tested *E. coli* cell solution. We measured

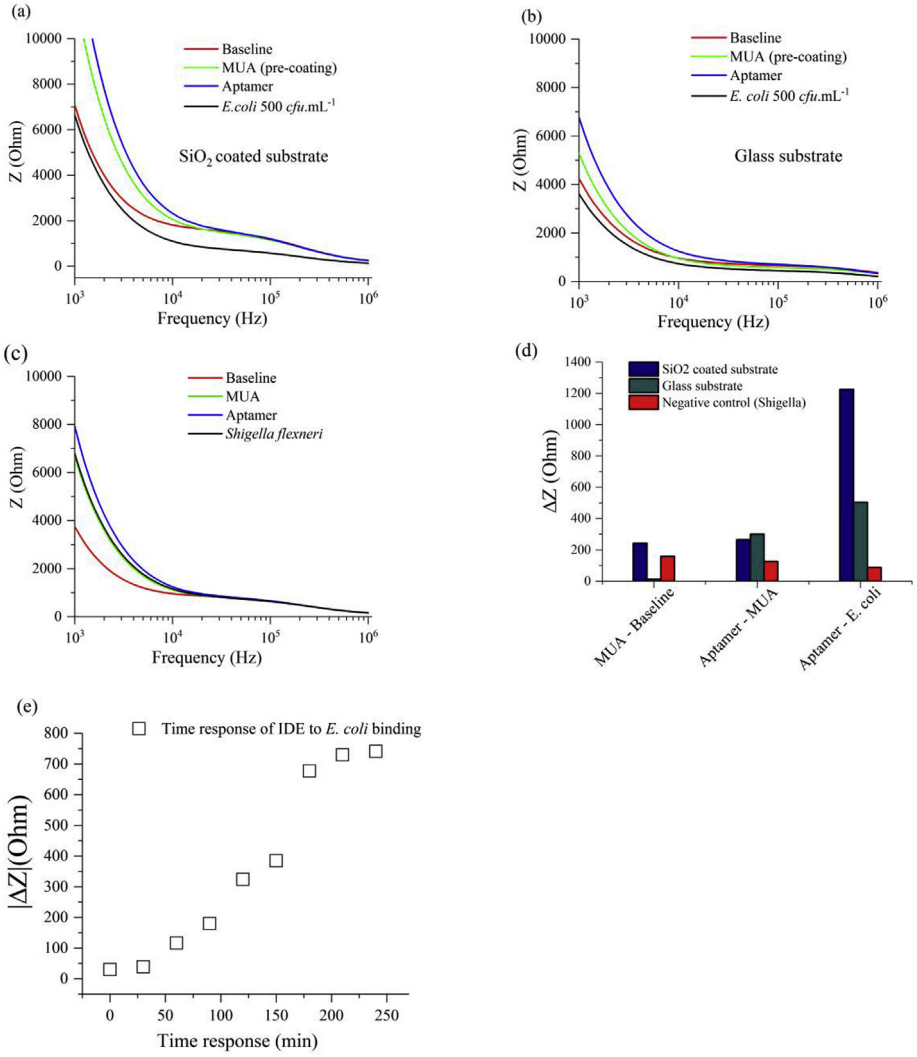

Fig. 3. Shows the impedance magnitude of the bare IDE made with silicon dioxide-coated substrate (a), and glass substrate (b) with that at different stages of electrode surface functionalization and after the addition of *E. coli* for detection, (c) the impedance magnitude of the bare IDE made with silicon dioxide-coated substrate and at different stages of surface functionalization and after the attachment of *Shigella flexneri* of 500 cfu mL^{-1} concentration as a negative control, (d) the calculated difference in the impedance magnitude at 10 kHz between two subsequent steps of surface functionalization, where we measured the impedance over the frequency range from 1 kHz to 1 MHz, and we pre-coated both of the silicon dioxide-coated substrate, and the glass substrate IDE with MUA 10 mM before functionalizing with aptamer. In the presented graphs, we used the *E. coli* solution of 500 cfu mL^{-1} concentration. (e)The time response of the *E. coli* OMP Ag1 Aptamer functionalized IDEs towards *E. coli* cells in water. The concentration of the *E. coli* OMP Ag Aptamer used in coating the IDEs was 5 μM, while the concentration of the *E. coli* solution was 250 cfu mL^{-1}. The experiments were repeated three times, and we presented the average values.

the ΔZ with *E. coli* concentration at 10 kHz and 100 kHz frequencies and found that the alteration in the ΔZ measured at 10 kHz is considerably significant compared to that at 100 kHz (the data not shown) implying that the sensitivity of the IDEs biosensor could vary depending on the utilized frequency. We previously had the same observation in the detection of metabolic protein with the assist of gold nanoparticles, where the sensitivity of the biosensor dramatically fall by measuring the ΔZ at 100 kHz instead of 10 kHz [1]. The doubling of the aptamer concentration to 5 and 10 μM used in the surface functionalization of the IDEs produced a linear increase in the ΔZ with *E. coli* cell increase over the range of the tested concentrations from 25 to 1000 cfu mL^{-1} as shown in Fig. 4 ((a), the red circle) and 4 ((a), the blue triangle), respectively. By measuring ΔZ at 10 kHz, the linear augment has a slope of 1.73 and 2.15 Ohm/(*cfu*.mL^{-1}), which represents the sensitivity of the sensor device, while it significantly drops about one order of magnitude to 0.16 and 0.18 Ohm/(*cfu*.mL^{-1}) at 100 kHz for 5 and 10 μM aptamer-probe concentrations, respectively, the data not shown. This drop in the slope implies that the frequency used in the measurement has a vital role here in determining the sensitivity of the IDEs sensor. On the other hand, the insignificant change in the slope with increasing the concentration of the aptamer-probe from 5 to 10 μM indicates that the optimal concentration of the probe for the tested concentration range of the *E. coli* cells has been achieved, and there is no need for a further increase in the used probe amount. We believed that the morphology of the electrode might contribute to identifying the optimal concentration of the aptamer probe. Here the IDE has a larger surface area exposed to the reaction medium due to its microstructure, and consequently it needs a higher aptamer concentration to efficiently cover the interface area. In addition, the volume of the solution and the electrochemical techniques used in the detection experiment might have an impact on the aptamer concentration. An OMP aptamer concentration of 0.02 μM was used in coating conventional gold electrode, and *E. coli*

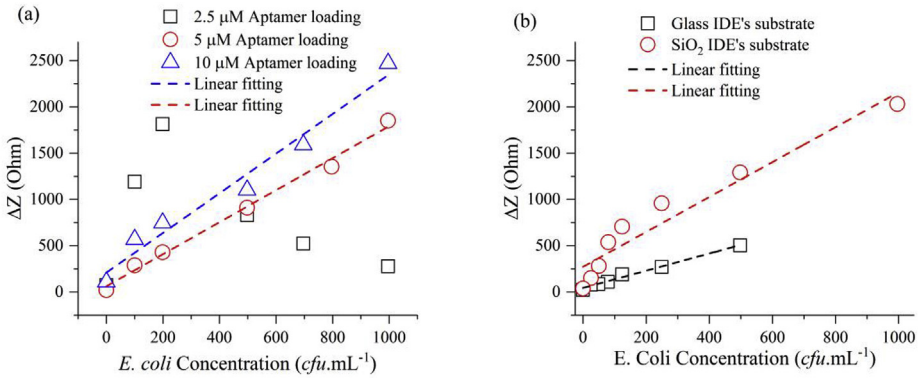

Fig. 4. (a) Representing the variation in the difference of the impedance magnitude ΔZ by changing the *E. coli* cells concentration at different Aptamer-probe concentrations coating the IDEs: (black square) 2.5, (red circle) 5.0, and (blue triangle) 10.0 μM. We selected silicon dioxide-coated wafers as the substrate for fabricating the IDEs. All IDEs were precoated with 10 mM MUA before the deposition of the Aptamer solutions. The sensor's response was measured at frequency 10 kHz. (b) Exemplifying the variation of the ΔZ with changing the concentration of the *E. coli* cells using different material substrates in the fabrication of the IDE, the glass (black square), and the SiO_2 coated silicon wafer (red circle). The sensitivity of the sensor device is represented by measuring the slope of the ΔZ with the test range of *E. coli* concentrations. Here, the concentration of the *E. coli* OMP Ag1 Aptamer is set at 5 mM, and the IDEs were pretreated with 1 mM of MUA. We repeated the sensing experiments three times and presented the average values. (For interpretation of the references to colour in this figure legend, the reader is referred to the Web version of this article).

was detected by faradaic impedance spectroscopy (FIS) using a 100 mL electrochemical cell [38]. The same OMP aptamer concentration (0.02 μM) was employed in the detection of *E. coli*, and a range of concentrations from 2×10^{-3} to 0.2 μM were tested [37]. In the studies, IDEs were tested using a 100 mL solution to detect the presence of the *E. coli*. Based on such results, we did not test higher or lower concentrations of the aptamer in the functionalization of the IDE as both of the 5 and 10 μM concentration solutions gave a linear increment in the ΔZ when increasing the tested concentration of the *E. coli* in the studied range.

2.3. The effect of the substrate electrical properties

The dielectric constant of the substrate material used in the fabrication of the IDEs affects its capacitance properties and consequently influences the sensitivity of the impedance-based sensor. By careful selecting of the IDEs' materials, it is possible to manipulate the sensitivity of the impedance-based sensor. For studying the impact of the variation in the material's dielectric constant on the sensing of the *E. coli*, we selected glass and SiO_2 coated wafer substrates to fabricate the IDEs. We followed the variation induced in the difference in the impedance magnitude (ΔZ) by changing the concentration of the added *E. coli* cells for each IDE. For both of IDEs made from glass and SiO_2 coated silicon wafer, ΔZ increases with increasing the added *E. coli* cells at 10 kHz frequency, as shown in Fig. 4 ((b), the black square) (a) and 4 ((b), red circle), respectively. Compared with that of the glass IDEs, the variation in the ΔZ of the SiO_2 coated wafer IDEs is significantly surpassing. The slope of the disparity in the ΔZ with changing the *E. coli* cells concentration is 1.89, and 0.9 Ohm/(*cfu*.mL^{-1}) for SiO_2 coated wafer and glass IDEs, respectively, which represents the significant impact of the substrate material of the IDEs on the sensitivity of the resulting sensors. The influence of the substrate material on the sensitivity of the IDEs sensors could arise from the dielectric properties of the material, where the dielectric constant of the glass and SiO_2 is 5–10 and 3.7–4.1, respectively. The limit of detection (LOD) in the case of SiO_2 coated wafer substrate is 8 cfu mL^{-1}, while it is 19 cfu mL^{-1} when we use glass as a substrate to fabricate IDEs. It is worth mention that the value of the dielectric constant of the SiO_2 coated layer depends on the deposition protocol [39]. The capacitance of the IDEs' substrate material is contingent on its dielectric constant, where the increment of the dielectric constant increases the capacitance. However, the capacitance is inversely proportional to the impedance of the fabrication substrate, as described by Equation (1) [40,41].

Consequently, the rise in the dielectric constant impairs the impedance caused by the substrate. As the net non-faradaic impedance of the IDEs consists of resistive and capacitance components and considering the sum of the impedance arises from the analyte, electrolyte solution droplet, and the parasitic impedance of the substrate, its value is significantly affected by the capacitance of the IDEs substrate as described in Equation (2). By reducing the parasitic impedance of the IDEs substrate, the value of the net impedance drops, which could negatively affect the value of the ΔZ at the same *E. coli* cell concentrations range. This destructive influence on the ΔZ could explain the diminishing of the IDEs sensors sensitivity by changing the substrate material from SiO_2 coated wafer to the glass.

$$Z_{par} = \frac{1}{j\omega Cpar} \tag{1}$$

$$Z_{net} = \left(R_{series} + 2Z_{dl})||(\frac{1}{j\omega Cgeo})||(Z_{par}\right) \tag{2}$$

Z_{par} and C_{par} are the parasitic impedance and the parasitic capacitance of the IDEs fabrication substrate, while R_{series} and C_{geo} represent the resistance of the solution and the geometric capacitance of the droplet, respectively, and Z_{dl} represents the double layer impedance.

2.4. The effect of SAM morphology

The usage of the SAM in the functionalization of the IDEs' surface is well-known by adding chemical affinity to the surface as well as reducing the nonspecific binding effect through the application of a bilayer [42]. We explored the effect of the molecular composition and the generated topography of the formation of SAM from the carboxy aliphatic thiol compounds on top of the IDEs' surface as a method to reduce the nonspecific binding and endow chemical activity, based on the sensitivity and the performance of the *E. coli* IDE sensor. To achieve this goal, we prepared a series of carboxy aliphatic thiol mixtures with different molar compositions of 11-MUA and 16-MDA and employed them to form SAMs on the IDE surfaces to endow chemical affinity to bond with the Aptamer-

probe. We prepared five chips where each was coated with only one mixture or single carboxy aliphatic thiol compounds and followed the variation of the ΔZ along with the tested range of the *E. coli* cell concentrations after the functionalization with OMP Ag1 aptamers. The slope of the ΔZ with the concentration of the *E. coli* as a representative of the IDE sensor sensitivity dramatically drops from 1.8 to 0.4 Ohm/(*cfu*.mL^{-1}) by introducing 10% 16-MDA to the carboxy aliphatic thiol mixture with 11-MUA (90%) as shown in Fig. 5 (black square) and 5 (black circle), respectively. The LOD shifts from 9 to 45 cfu mL^{-1} by introducing 10% of 16-MDA to the carboxy aliphatic thiol mixture used in the IDE surface modification. By increasing the ratio of the 16-MDA to 50% in the mixture the slope slightly increases to 0.77 Ohm/(*cfu*.mL^{-1}) before falling again to 0.29 Ohm/(*cfu*.mL^{-1}) with continuous increasing of the 16-MDA ratio up to 90%, as presented in Fig. 5 (red square) and 4 (red circle), respectively. While using 16-MDA alone as a surfactant for producing the SAM reduces the slope by about ten times to 0.23 Ohm/(*cfu*.mL^{-1}) compared with that in the case of using 11-MUA molecules, as depicted in Fig. 5 (blue square). The 16-MDA modified IDEs showed a negative response with lower concentrations of *E. coli* cells (25, and 50 cfu mL^{-1}), where ΔZ has negative values. This negative response implies the role of the 16-MDA in diminishing the detection limit and the sensitivity of the IDEs sensors. The LOD values fluctuated with changing the composition of the carboxy aliphatic thiol mixture and became 70 cfu mL^{-1} when we solely used 16-MDA as a surfactant to modify the IDEs' surface. As observed, the change in the aliphatic chain length or the molar ratio of the carboxy aliphatic thiol mixture creates a sizeable impact on the sensitivity and the LOD of the IDE sensor, whereas adding five carbon atoms to the aliphatic chain decreases the sensitivity one order of magnitude. Also, changing the molar ratio of the carboxy aliphatic thiol compounds mixture by introducing 10% 0f 16-MDA induces a considerable decrease in the sensitivity in comparison with using 11- MUA alone as a surfactant. However, the inclusion of 10% 11-MUA produces a trivial impact on the sensitivity of the IDE sensor in comparison with using 16-MDA alone as a surfactant in the formation of the SAM. Both of the 11-MUA and 16-MDA possess a terminal carboxylic group which endows the affinity to the IDEs surface to bind the amine terminal group of the OMP Ag1 aptamer through EDC/NHS biochemical conjugation. We believe that using carboxy aliphatic thiol as a linker is in general preferable to anchor the aptamer to the gold digits of the IDEs to avoid overusing aptamers terminated with thiol groups. SAM formed from the carboxy aliphatic thiol molecules could effectively reduce the nonspecific adsorption effect. Changing the aliphatic chain length or molecular composition of the SAM precursor solution changes the composition of the SAM, and consequently changes the topographical roughness of the resulted monolayer. This alteration in the topography of the SAM results in a turmoil for the molecular arrangement and orientation of the OMP Ag1 aptamer molecules, which might influence the attachment with the outer membrane protein of the *E. coli* and hence reduces the affinity. The impact of the aliphatic chain length and the composition of the SAM precursor solution on the topographic roughness of the monolayer is presented in detail in the supporting information (Fig. S3).

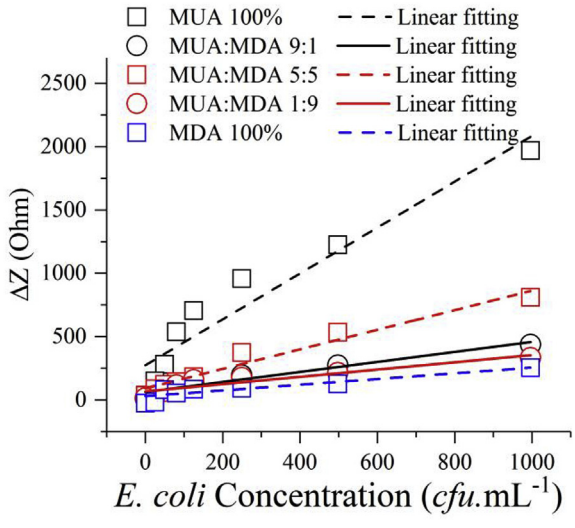

Fig. 5. The variation in the IDE sensitivity (slope of the ΔZ with *E. coli* concentrations) with the change in the molar composition of the carboxy aliphatic thiol mixture precoating layer. The concentration of the *E. coli* OMP Ag1 Aptamer used here is 5 μM. We tested the IDE sensor with an *E. coli* concentration range from 25 to 996 cfu over SiO_2 coated silicon wafer IDEs' substrate. We measured the ΔZ at frequencies 10 kHz using (black square) MUA 10 mM, (black circle) MUA 9 mM and MDA 1 mM, (red square) MUA 5 mM and MDA 5 mM, (red circle) MUA 1 mM and MDA 9 mM, and (blue square) 10 mM of MDA to form the SAM before OMP Ag1 aptamer functionalization. We repeated the sensing experiments three times and presented the average values. (For interpretation of the references to colour in this figure legend, the reader is referred to the Web version of this article.)

In each of the above experiments, we measured the ΔZ at two different frequencies 10 kHz and 100 kHz (data not shown for 100 kHz). By comparing the sensitivity at 10 and 100 kHz, it drops by around 80% for most carboxy aliphatic thiol compositions when we measured at 100 kHz, except that when 11-MUA is the surfactant where it falls by 66%. This was the same behavior we observed before with changing the OMP Ag1 aptamer concentration and the electrode substrate material.

The development of a portable and handy sensor for *E. coli* has great potential in various fields, including water resources quality monitoring, food safety, agriculture, and pharmaceutical. The design of the sensor should fulfill certain requirements to compete with the traditional analytical techniques such as easy to fabricate and operate, working under ambient conditions, and finally, affordable operational cost without waiving high sensitivity and low LOD. Few attempts have employed the advantages of the aptamer and IDEs to develop a portable and endure sensor for *E. coli*. Comparing to the design proposed by Sergi Brosel-Oliu and his team [37] to build an impedimetric sensor for label-free detection of *E. coli* bacteria, our developed sensor device relied on the functionalization of the metal fingers electrodes instead of the gap between the electrodes. This functionalization protocol located the *E. coli* cells on the top of the metal electrodes rather than in between and highly away from the electrodes, which might explain the low LOD (9 cfu) for our design compares to the higher LOD (100 cfu) for the Sergi's design. Despite the similarity in the general design, but we used different aptamer probe (*E. coli* OMP Ag1) and various materials in the fabrication of the IDEs (gold instead of $TaSi_2$), and the sample compartment in our design has a volume of 30 μL which allow to take minimal amount of the tested solution and help in miniaturizing the sensor size. It is worth to mention that, our chip has eight IDEs of 3 mm^2 square area each, which allows running eight different tests using single chip by aligning and placing PDMS cover with eight wells on the top of the IDEs chip and that would lower the cost per test. We also investigated the role of the IDE's substrate materials on the sensitivity of the fabricated sensor, which assists in understanding the mechanism of non-faradaic sensing of *E. coli*. Using gold as an electrode finger materials give significant flexibility in surface functionalization, and that allows anchoring the aptamer to the electrode digits surface.

The detection of the *E. coli* using a non-faradaic impedance IDE sensor depends on its electrical characteristics as a capacitor. The

non-conductive *E. coli* cell membrane surrounds the periplasmic space, cytoplasm, and its constituents as charged conductive species, which emulates the capacitor structure. Simulation studies have been elaborated using either double or triple-layer spheroidal models to estimate the dielectric properties of *E. coli* cell components [36,43]. Hence, the sensing of the *E. coli* by non-faradaic impedance spectroscopic techniques after anchoring to an IDE's surface by the OMP Ag1 aptamer as a surface effect is resulting from its impact on the double layer capacitance C_{dl}, which is predominant at low-frequency ranges [44,45]. At a higher frequency range, the medium capacitance commands the impedance of the IDEs, which limits the effect of the *E. coli* presence on the impedance magnitude. The capacitive nature of the *E. coli* contributes to the impedance of the IDEs at lower frequency range more than that at a higher frequency range, which explains the higher sensitivity of the IDEs sensor to the *E. coli* cells at the lower frequency (10 kHz) regardless the other parameters. The dielectric properties of the substrate used in the fabrication of the IDEs would contribute to the electric field of the microelectrode array, which in turn could influence the sensor sensitivity. The IDE chips that were made from glass and SiO_2 coated silicon wafer had the same fabrication procedures and identical morphology, but they had a significant difference in the sensitivity. This variation in the sensitivity arose from the variance in the dielectric constant of the substrate material. Leveraging the biological stability of the DNA-aptamer as a probe for detecting *E. coli* would assist in building biosensors that could support outdoor environmental activities such as water resource surveillance surpassing that which was built on Antibody probe-based sensors. However, it is pivotal to take into account the role of the molecular structure, mixture composition of the surfactant molecules, and their impact on the molecular assembly on the top of the microelectrodes in determining the IDEs sensors sensitivity and other properties. The same aptamer was successfully employed during the electrochemical detection of the outer membrane protein of two different strains of *E. coli* (O157:H7 and 8739), and it showed high specificity for *E. coli* BL21. Therefore, we can conclude an *E. coli* outer membrane protein-specific aptamer is a good candidate as a general probe to develop a portable electrochemical sensor for *E. coli* and has great potential in different applications.

3. Conclusion

In summary, we developed IDE chips with the capability to be employed as a biosensor for environmental and potable water monitoring applications. The pliability of choosing the electrode materials, and bioengineering their surface functionality was exploited to detect *E. coli* bacteria. *E. coli,* as a Gram-negative anaerobic bacterium, usually is available in human and animal intestines, but some strains are pathogenic and cause a severe infection. The detection of *E. coli* in potable water, water sources, and food products could provide an effective surveillance system for health protection and food safety. We used impedance-based electrochemical detection using IDEs to sense the existence of *E. coli* in potable water. We evaluated the effect of the relative permittivity (dielectric constant) of the IDEs substrate material, the molecular stacking of the carboxy aliphatic thiol linker, and the concentration of the aptamer-probe on the sensitivity and the detection limit of the developed *E. coli* biosensor. By optimizing the fabricating substrate material, the surfactant used to activate the IDEs surface, and the concentration of the aptamer-probe, it is possible to build a portable biosensor device for detecting the *E. coli* bacteria with high sensitivity.

4. Materials and methods

4.1. Materials

1-Mercapto-11-undecanoic acid 97% (11-MUA), 2-(*N*-morpholino) ethanesulfonic acid (MES), N-(3-(dimethylamino) propyl)-N-ethylcarbodiimide hydrochloride (EDC), N-hydroxysuccinimide 98% (NHS), Magnesium chloride, TRIS hydrochloride**,** Ethylenediaminetetraacetic acid (EDTA**),** Luria Agar, Luria broth**,** Ethanol (100%), Disodium hydrogen phosphate, and monosodium hydrogen phosphate were purchased from Sigma-Aldrich Canada Co. (Oakville, Ontario) and were used without further purification. *Escherichia coli* Outer Membrane Protein Ag1 (*E. coli* OMP Ag1) was purchased from OTCBiotech, where it is amine terminated oligonucleotide at 5′ end, and its sequence is 5′-NH_2-ATCCGTCACACCTGCTCT-ACGGCGCTCCCAACAGGCCTCTCCTTACGGCATATTATGGTGTTGGCTCCCGTAT-3′. We selected this aptamer because of its high recognition affinity to the outer membrane protein of several strains of *E. coli* bacteria such as O157:H7 and 8739 [35, 37, 38, 46]. Ultrapure water (18.2 MΩ/cm) obtained from Millipore equipment (Mili-Q water) was used for samples preparation and washing.

4.2. Apparatus

All electrochemical measurements were performed with an Electrochemical Impedance Spectroscopy benchtop potentiostat/galvanostat SP-200 controlled by EC lab software from BioLogic Science instrument Inc (Knoxville, Tennessee) by applying a 10 mV sinusoidal excitation perturbation at 0 V DC in the frequency range of 10 Hz to 1 MHz. A Zeiss Sigma Field Emission Scanning Electron Microscope (FESEM) and a digital optical microscope VHX-700F from KEYENCE Canada Inc. (Mississauga, Ontario) were used for imaging and estimating the number of *E. coli* captured on the surface of the IDEs. We also used a hemocytometer and Motic AE 31 an inverted biological microscope (Carlsbad, California), to count the number of *E. coli* cells in the tested solution. A Veeco di multimode V atomic force microscope (AFM) to follow the surface chemical bioengineering of the IDEs at different functionalization stages.

Custom designed IDE sensor chips were fabricated on silicon wafers with around 500 nm thermal oxide following a standard photolithography process flow involving sputter deposition of chromium (10 nm) and gold (100 nm), photoresist and photomask pattern transfer followed by the development, and reactive ion plasma etching. Each sensor chip has eight IDEs units of 3 mm^2 square area and 168 digit pairs with length, width, thickness, and a gap of 3 mm, 4 μm, 110 nm, and 4 μm respectively. A PDMS mask with eight wells of 3 mm^2 was designed and fabricated in the lab that fits the IDEs to assist in the functionalization of each IDE's surface without affecting the other wells on the same chip. The digital images of the IDE chips made with SiO_2 coated substrate, glass, and the PDMS cover were presented in Fig. S4. The PDMS mask allows independent and localized modification of each IDE on a sensor chip with any desired modifying solution.

4.3. Methods

4.3.1. IDEs cleaning, pre-treatment, and functionalization

Before the surface functionalization of the IDEs, they were cleaned by sonicating in acetone followed by isopropanol for 5 min each to remove the residue of the photoresist material. Then the IDE chips were rinsed with Milli-Q water and then dried with a stream of nitrogen. The pre-cleaned IDE chips were functionalized in sequential reaction steps by the addition of different solutions using the PDMS mask to cover the IDE chips and separate each IDE. Following successive functionalization steps, the IDEs were washed

with ethanol and 10 mM PBS at pH 7.4 and Milli-Q. To achieve a self-assembled monolayer (SAM) with the distal carboxylic acid group on the surface of the IDEs, two different carboxy aliphatic thiol compounds 11-MUA, and 16-MDA were used separately or in a mixture with different molar ratios. An example of the SAM coating: 50 μL of 11-MUA was added to each well of the PDMS cover attached to the IDE chip and incubated for 8 h at 4 °C. We repeated the same step using the other carboxy aliphatic thiol compound and mixtures. The carboxyl groups of the SAM-modified IDEs were activated by incubating with 50 μL of 0.1 M EDC and 0.05 M NHS freshly prepared in a MES buffer for 30 min, before adding the *E. coli* OMP Ag1 aptamer solution. 50 μL of 5 μM E. *coli* OMP Ag1 aptamer was added to each well of the PDMS cover and incubated for 4 h to complete the functionalization of the IDEs. After every step of surface modification, electrode washing was performed with 10 mM PBS, and Milli-Q.

4.3.2. E. coli BL21 cell culture and aptamer optimization

E. coli BL21 strain was grown on a Luria agar plate overnight at 37 °C. A loop full of bacterial culture was transferred from plate to 10 mL Luria broth and incubated at 37 °C in a shaking incubator until its optical density estimated spectrophotometrically reaches 0.7A at 650 nm. We measured the colony-forming unit (*cfu*) per mL of *E. coli* bacteria using the hemocytometer and optical microscope and prepared a range of *E. coli* concentrations from 25 to 1000 cfu mL^{-1}. Across the experiments, we used non-pathogenic *Shigella flexneri* of 500 cfu mL^{-1} concentration as a negative control sample referred to as 0 cfu mL^{-1} E. *coli*.

E. coli OMP Ag1, 100 mol, with 5′Amine was spun down briefly to avoid loss of the aptamer pellet. The stock aptamers were entirely dissolved to the desired stock concentration of 100 μM in 10 mM TE buffer by stirring over 30 min. Then aliquot stock aptamers were stored at −20 °C until further use.

For the dilution, aptamers were dissolved in 1X PBS. Aptamers are stable at a neutral pH range (7.0–8.0). For the proper folding of the aptamer structure in the buffer, they were heated at 95 °C for 5 min and slowly cooled at room temperature for 15 min in the presence of the 2^{+} ion magnesium. The addition of 2^{+} ion magnesium in the buffer is critical for maintaining a proper aptamer structure.

4.3.3. Non-faradaic impedance measurements

After each step of IDE surface functionalization, we measured the non-faradaic impedance using measuring buffer (PBS buffer 10^{-6} M) as an electrolyte in the range of frequency from 1 kHz to 1 MHz and applied current of 100 mA. We followed the same protocol when we measured the impedance of the IDE chips after the binding of the *E. coli* to the IDEs' surfaces. We placed the PDMS cover over the IDE chip by adjusting one well centering on the top of each IDE to hold the measuring solution. Across experiments, the impedance measurement was performed by placing 30 μL of the measuring electrolyte or the analyte solution in each well of the PDMS cover. All impedance sensing experiments were repeated three times, and we presented the average values.

4.3.4. Detection of E. coli

Determining the sensitivity of the biosensor toward the *E. coli* proceeded through choosing *E. coli* BL21 as an example and preparing a series of *E. coli* BL21 solutions with different concentrations from 20 to 1000 cfu mL^{-1} and measuring the impedance response. After completing the functionalization of the IDEs with the aptamer, 30 μL of test solution containing *E. coli* was placed on the top of each IDE in the chip surrounded by the PDMS cover. We left the *E. coli* solution incubated for 1 h to give the chance to bind with the IDE surface-functionalized with aptamer except in the experiment we measure the time response as we change the incubation time. After that, we removed the *E. coli* solution and washed the IDEs three times with Milli-Q ultrapure water before adding the impedance measuring buffer (PBS 10^{-6} M) following the procedures mentioned above. We repeated the same steps for all *E. coli* concentrations solutions, all tested IDEs (SiO_2 coated silicon substrates and the glass substrates), and all carboxy aliphatic thiol mixtures.

Declaration of competing interest

The authors declare that they have no known competing financial interests or personal relationships that could have appeared to influence the work reported in this paper.

CRediT authorship contribution statement

Gaser N. Abdelrasoul: Writing - original draft. **Afreen Anwar:** Writing - original draft. **Scott MacKay:** Conceptualization, Methodology. **Marcus Tamura:** Methodology, Validation. **Manzoor A. Shah:** Funding acquisition. **Damase P. Khasa:** Funding acquisition. **Ruth R. Montgomery:** Writing - review & editing. **Albert I. Ko:** Writing - review & editing. **Jie Chen:** Writing - original draft.

Acknowledgments

The authors would like to thank the Canada-India Research Centre of Excellence (IC-IMPACTS) for financial support.

Appendix A. Supplementary data

Supplementary data to this article can be found online at https://doi.org/10.1016/j.aca.2020.02.004.

References

[1] G.N. Abdelrasoul, S. MacKay, S.Y. Salim, K.P. Ismond, M. Tamura, C. Khalifa, E. Mannan, D. Lin, T. Mandal, R.R. Montgomery, D.S. Wishart, J. Chen, R.G. Khadaroo, ACS Sens. 3 (2018) 2296–2302.
[2] R. Radhakrishnan, I.I. Suni, C.S. Bever, B.D. Hammock, ACS Sustain. Chem. Eng. 2 (2014) 1649–1655.
[3] C.K. Ho, A. Robinson, D.R. Miller, M.J. Davis, Sensors 5 (2005) 4.
[4] I.C. Justino, C.A. Duarte, A.T. Rocha-Santos, Sensors 17 (2017).
[5] G.N. Abdelrasoul, F. Pignatelli, I. Liakos, R. Cingolani, A. Athanassiou, Compos. B Eng. 149 (2018) 178–187.
[6] R. Maalouf, C. Fournier-Wirth, J. Coste, H. Chebib, Y. Saïkali, O. Vittori, A. Errachid, J.-P. Cloarec, C. Martelet, N. Jaffrezic-Renault, Anal. Chem. 79 (2007) 4879–4886.
[7] S. Kim, G. Yu, T. Kim, K. Shin, J. Yoon, Electrochim. Acta 82 (2012) 126–131.
[8] F. Abbasian, E. Ghafar-Zadeh, S. Magierowski, Bioengineering 5 (2018).
[9] Y. Wang, Z. Ye, Y. Ying, Sensors 12 (2012).
[10] L.C.T. Shoute, A. Anwar, S. MacKay, G.N. Abdelrasoul, D. Lin, Z. Yan, A.H. Nguyen, M.T. McDermott, M.A. Shah, J. Yang, J. Chen, X.S. Li, Sci. Rep. 8 (2018) 12396.
[11] S.-Y. Wu, J. Hulme, S.S.A. An, BioChip J. 9 (2015) 173–181.
[12] D. Mendes Silva, L. Domingues, Ecotoxicol. Environ. Saf. 113 (2015) 400–411.
[13] A.K. Deisingh, M. Thompson, J. Appl. Microbiol. 96 (2004) 419–429.
[14] M. Xu, R. Wang, Y. Li, Talanta 162 (2017) 511–522.
[15] A. Güner, E. Çevik, M. Şenel, L. Alpsoy, Food Chem. 229 (2017) 358–365.
[16] M. Xu, R. Wang, Y. Li, Talanta 148 (2016) 200–208.
[17] R.-R. Hu, Z.-Z. Yin, Y.-B. Zeng, J. Zhang, H.-Q. Liu, Y. Shao, S.-B. Ren, L. Li, Biosens. Bioelectron. 78 (2016) 31–36.
[18] H. Stender, A.J. Broomer, K. Oliveira, O. Perry, H. Keefe, J.J. Hyldig-Nielsen, A. Sage, J. Coull, Appl. Environ. Microbiol. 67 (2001) 142.
[19] P. Ramakrishnan, J.J. Tabor, ACS Synth. Biol. 5 (2016) 733–740.
[20] N.T. Ong, E.J. Olson, J.J. Tabor, ACS Synth. Biol. 7 (2018) 240–248.
[21] J. Chen, S.D. Alcaine, Z. Jiang, V.M. Rotello, S.R. Nugen, Anal. Chem. 87 (2015) 8977–8984.
[22] L. Heijnen, G. Medema, Water Res. 43 (2009) 3124–3132.
[23] I.U.H. Khan, V. Gannon, R. Kent, W. Koning, D.R. Lapen, J. Miller, N. Neumann, R. Phillips, W. Robertson, E. Topp, E. van Bochove, T.A. Edge, J. Microbiol. Methods 69 (2007) 480–488.

[24] D. Wang, J. Chen, S.R. Nugen, Anal. Chem. 89 (2017) 1650–1657.
[25] F. Li, Z. Yu, H. Qu, G. Zhang, H. Yan, X. Liu, X. He, Biosens. Bioelectron. 68 (2015) 78–82.
[26] Y. Guo, Y. Wang, S. Liu, J. Yu, H. Wang, Y. Wang, J. Huang, Biosens. Bioelectron. 75 (2016) 315–319.
[27] M. Barreiros dos Santos, J.P. Agusil, B. Prieto-Simón, C. Sporer, V. Teixeira, J. Samitier, Biosens. Bioelectron. 45 (2013) 174–180.
[28] M. Mallén-Alberdi, N. Vigués, J. Mas, C. Fernández-Sánchez, A. Baldi, Sens. Bio-Sens. Res. 7 (2016) 100–106.
[29] Y. Li, R. Afrasiabi, F. Fathi, N. Wang, C. Xiang, R. Love, Z. She, H.-B. Kraatz, Biosens. Bioelectron. 58 (2014) 193–199.
[30] M. Kim, T. Jung, Y. Kim, C. Lee, K. Woo, J.H. Seol, S. Yang, Biosens. Bioelectron. 74 (2015) 1011–1015.
[31] M. Xu, R. Wang, Y. Li, Analyst 141 (2016) 5441–5449.
[32] M.R. Akanda, V. Tamilavan, S. Park, K. Jo, M.H. Hyun, H. Yang, Anal. Chem. 85 (2013) 1631–1636.
[33] Y. Zhang, B.S. Lai, M. Juhas, Molecules 24 (2019) 941.
[34] S. Marton, F. Cleto, M.A. Krieger, J. Cardoso, PloS One 11 (2016), e0153637.
[35] Y.-W. Zhao, H.-X. Wang, G.-C. Jia, Z. Li, Sensors 18 (2018) 2518.
[36] W. Bai, K.S. Zhao, K. Asami, Biophys. Chem. 122 (2006) 136–142.
[37] S. Brosel-Oliu, R. Ferreira, N. Uria, N. Abramova, R. Gargallo, F.-X. Muñoz-Pascual, A. Bratov, Sensor. Actuator. B Chem. 255 (2018) 2988–2995.
[38] R.B. Queirós, N. de-los-Santos-Álvarez, J.P. Noronha, M.G.F. Sales, Sensor. Actuator. B Chem. 181 (2013) 766–772.
[39] M. Katsumi, Jpn. J. Appl. Phys. 33 (1994) 1385.
[40] P. Dak, A. Ebrahimi, M.A. Alam, Lab Chip 14 (2014) 2469–2479.
[41] K. Hashimoto, K. Niwa, Electron. Commun. Jpn. Part II Electron. 72 (1989) 16–22.
[42] A.B. Steel, T.M. Herne, M.J. Tarlov, Anal. Chem. 70 (1998) 4670–4677.
[43] K. Asami, T. Hanai, N. Koizumi, Biophys. J. 31 (1980) 215–228.
[44] S.M. Radke, E.C. Alocilja, Biosens. Bioelectron. 20 (2005) 1662–1667.
[45] S.M. Radke, E.C. Alocilja, IEEE Sensor. J. 4 (2004) 434–440.
[46] J.G. Bruno, M.P. Carrillo, T. Phillips, C.J. Andrews, J. Fluoresc. 20 (2010) 1211–1223.